Characteristic jump in the electrical properties of a Pd/AlN/Si-based device on exposure to hydrogen

J. S. Thakur,[1,*] H. E. Prakasam,[1] Linfeng Zhang,[1] E. F. McCullen,[1] L. Rimai,[1] V. M. García-Suárez,[2] R. Naik,[3] K. Y. S. Ng,[4] and G. W. Auner[1]

[1]*Department of Electrical and Computer Engineering, Wayne State University, Detroit, Michigan 48202, USA*

[2]*Department of Physics, Lancaster University, Lancaster LA1 4YB, United Kingdom*

[3]*Department of Physics and Astronomy, Wayne State University, Detroit, Michigan 48202, USA*

[4]*Department of Chemical Engineering and Materials Science, Wayne State University, Detroit, Michigan 48202, USA*

(Received 15 June 2006; revised manuscript received 11 December 2006; published 6 February 2007)

The time-dependant current response of Pd/AlN/Si-based devices is investigated for different hydrogen concentrations. At a fixed applied voltage, the device current suddenly increases when hydrogen gas is turned on and the magnitude of this current shift varies with the hydrogen concentrations. Using first-principles simulations, the electronic structure of the Pd with different hydrogen concentrations in tetrahedric and octahedric positions is calculated. We find that when hydrogen loads the Pd metal, its Fermi energy changes, which affects the Fermi level of the Pd/AlN/Si device and thus its electrical response.

DOI: 10.1103/PhysRevB.75.075308 PACS number(s): 68.43.Mn, 68.65.Ac, 68.47.−b

I. INTRODUCTION

Recently the research activities for designing ultrasensitive hydrogen sensors have become quite widespread due to their growing demand in the areas of automobile, aircraft, and other bioindustries. Particularly, monitoring of emissions from high-temperature combustion systems or chemical systems poses tough challenges for designing sensors stable enough to withstand high-temperature conditions. For such areas, application of wide-band-gap semiconductor materials (e.g., AlN) in conjunction with Pd metal has become quite popular in metal/insulator/semiconductor (MIS) devices because of their tolerance to high temperatures and high sensitivity to hydrogen. It was found that the electrical properties of a field-effect transistor device[1–4] based on Pd metal, i.e., a palladium metal oxide semiconductor (Pd-MOS), were quite sensitive to hydrogen exposure. Later on, palladium-metal-based MIS devices have also been extensively developed[5,6] for hydrogen detection. These devices showed a very generic behavior when exposed to hydrogen gas: the capacitance of a device when measured against voltage showed a sudden increase[7] in its values when hydrogen was turned on, and a similar increase was also observed in the current when plotted against time. The magnitude of the jump in the electrical properties for a small amount of hydrogen exposure is directly related to the sensitivity of the device—an important parameter of a sensor. Although defects and other factors can influence the device response,[8,9] the origin of the jump—the most crucial characteristic of the electrical measurements—still remains unclear. The shift in the current and voltage has been related to the formation of the charge states or dipole at the insulator-semiconductor interface,[10] however, there is no direct method to measure these dipoles. In order that Pd-based MIS devices could be used for hydrogen sensing applications, it is important to understand whether this response is an intrinsic property of these MIS devices or an artifact of these charge states or dipole formation, which depends on the device preparation procedure and fabrication techniques.

In this paper, we experimentally investigate the time-dependent behavior of current in Pd/AlN/Si devices for different hydrogen concentrations. In electrical measurements of MIS devices, the Fermi level of the metal plays a very crucial role. In order to determine the microscopic mechanism for the variations in the electrical properties of these devices, we investigated the equilibrium electronic structure, particularly the density of states (DOS) function which measures the location of Fermi level, and variation in the lattice constant of Pd using *ab initio* calculations for different concentrations of hydrogen. These calculations showed that when hydrogen gas loads the Pd metal and occupies energetically favorable sites, the Fermi level of the Pd metal changes. The dynamically changing Fermi level of the Pd metal due to varying hydrogen concentration induces dynamical variations in the Fermi level of the MIS device and thus generates a hydrogen-concentration-dependent response in the electrical properties of these devices.

The paper is organized as follows: In Sec. II we discuss the experimental details used in the fabrication of the Pd/AlN/Si device and the current response as a function of time for different concentrations of hydrogen. The *ab initio* calculations and their results are presented in Sec. III. The role of PdH Fermi energy in the electrical response of the devices is discussed in Sec. IV.

II. EXPERIMENTAL DETAILS AND RESULTS

The AlN layer was deposited on *n*-type Si(111) by plasma source molecular beam epitaxy (PSMBE).[11] During the deposition of the AlN, the substrate was held at a negative bias of 10.0 V under a constant flow of 40 sccm of argon and 10 sccm nitrogen. Depositions were performed with the substrate heated to 600 °C. X-ray diffraction showed that the AlN films were highly textured, with *c* axis orientation normal to the film surface. Thickness measurements with a Gaertner manual null-ellipsometer showed that AlN films are

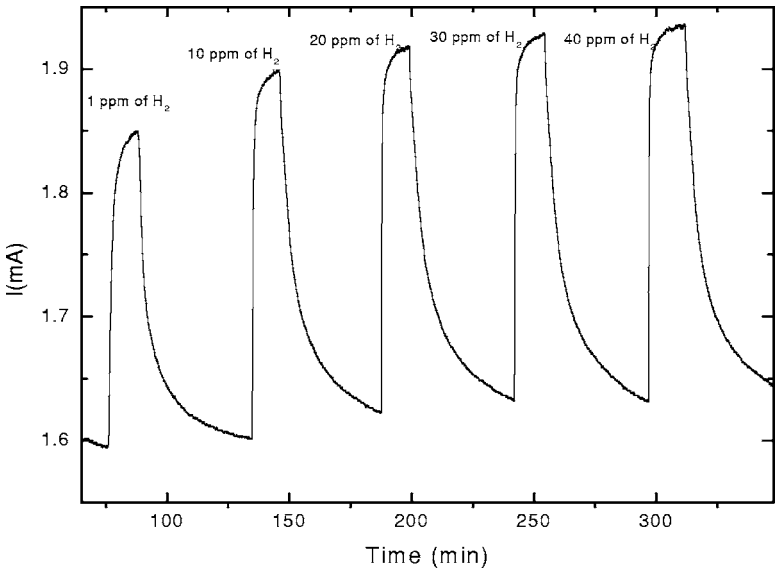

FIG. 1. The current response of the Pd/AlN/Si device to different values of hydrogen concentrations.

~500 Å thick. An Al back contact (3000 Å) and Pd (1000 Å) gates of 1.0 mm diameter were deposited by magnetron sputtering in a separate chamber, and the thicknesses were measured with a Dektak 3030 profilometer. Before we measure the device response for different flow rates of hydrogen, the system is initially purged for several hours with nitrogen gas in order to eliminate or minimize the presence of oxygen gas. All the hydrogen ppm values given in this paper are in the surrounding nitrogen flow; while the total flow rate is maintained constant. The electrical measurements were performed in a separate chamber and are described elsewhere.[12]

In a Pd metal, the absorbed hydrogen affects its electrical properties, e.g., Fermi level,[13] optical properties,[14] surface conductivity, or thermo power, etc. The changes in the electrical properties[1–4] due to variations in hydrogen concentration can be measured in terms of changes in the current or voltage values when Pd is interfaced with a semiconductor to form a Pd/AlN/Si type of heterostructure device. These changes which are directly related to the concentrations of hydrogen could be used to monitor the level of hydrogen concentration in a particular environment. Figure 1 shows a typical current, $I(t)$, vs time, t, response of the Pd/AlN/Si device when exposed to different hydrogen ppm rates at 75 °C temperature. For a given hydrogen concentration, the device shows two main responses when hydrogen is turned on: (1) the transient response where current increases rapidly with time, and (2) the steady-state response where current has acquired a constant value. During the turned-off cycle, the current first drops suddenly at the turn-off time and then gradually goes to its original value. The transient responses of the device are not symmetric for the turn-on and turn-off cases. Since the hydrogen diffusion time through the bulk is very short, the characteristic time for the current to acquire a steady-state value depends mainly on chemisorptions/desorption kinetics of H_2 molecules at the Pd surface and the adsorption/desorption processes at the Pd/AlN interface. These two processes at the surface and interface are dynamically coupled to each other.[8,10] Pd with a clean surface has nearly 100% adsorption rate for hydrogen, but other factors, like evaporation, impurities in the gases, and charging and discharging of the Pd with hydrogen can change the surface and bulk properties and thus influence the adsorption rate and equilibrium state of the device.

The most interesting feature of the current response is a sudden jump in the values of $I(t)$ when hydrogen is turned on. This feature has also been observed in other devices[15] where the electrical response to hydrogen exposure is measured either in terms of current or capacitance. The steady-state value of the current depends on the ppm value and it increases monotonically with increasing ppm values. The spike in the current or capacitance value, when hydrogen is turned on, is a ubiquitous behavior of the Pd/insulator/semiconductor or Pd-alloy-based MIS devices, and this phenomenon has been thought to have a potential for designing sensitive hydrogen sensors.

Hydrogen adsorption at the surface mainly happens at three different geometrical sites, normally denoted as β_1, β_2, and β_3 with energy around 0.26 eV, 0.40 eV, and 0.52 eV per atom, respectively.[16] The thermal desorption spectroscopy showed[17] that for low exposures of hydrogen and for temperatures between 320 K and 340 K, the only adsorption observed is from the β_3 state. Our experiments are performed at constant temperature of 348 K, so we expect that most of the hydrogen adsorption is occurring at β_3 sites. Molecular hydrogen after adsorbing on the Pd surface dissociates into atomic hydrogen, which then diffuses through the bulk, occupying the available tetrahedral sites when temperatures are low. At higher temperatures, however, hydrogen atoms begin to load the octahedral sites. Depending on the temperature and value of atomic concentration ratio $[N_H]/[N_{Pd}]$, the solid solution of the Pd-H system can exist in one of three phases, α, $\alpha+\beta$, and β. At room temperature for low dosages of hydrogen, $0<[N_H]/[N_{Pd}]<0.05$, the α phase of PdH is the most stable. The β phase gets stabilized[18] only at higher hydrogen concentrations, $[N_H]/[N_{Pd}]>0.6$, and this phase can exist even at low temperatures. The hydrogen partial pressure in our experimental setup is less than atmospheric pressure, and we expect that our Pd-H system is in the α phase. In order to understand the behavior of these devices,

TABLE I. Lattice constant and Fermi energy of the Pd/H system calculated with a DZP basis set and LDA for different hydrogen concentrations. Octahedric 1 and octahedric 2 in the $Pd_{16}H_2$ cases correspond to two possible configurations of the hydrogen in the unit cell (separated 1.97 and 2.79 Å, respectively).

System	Lattice constant (Å)	Fermi energy (eV)
PdH (tetrahedric)	4.19	−4.48
PdH (octahedric)	4.08	−4.17
Pd_4H (tetrahedric)	3.99	−4.55
Pd_4H (octahedric)	3.96	−4.44
$Pd_{16}H_2$ (octahedric 1)	3.94	−4.36
$Pd_{16}H_2$ (octahedric 2)	3.94	−4.36
$Pd_{16}H$ (tetrahedric)	3.93	−4.34
$Pd_{16}H$ (octahedric)	3.93	−4.32
$Pd_{32}H$ (tetrahedric)	3.92	−4.33
$Pd_{32}H$ (octahedric)	3.91	−4.31
Pd	3.90	−4.27

we focus on determining the changes in the electronic properties, particularly the Fermi energy, of Pd when hydrogen loads the Pd bulk and occupies different lattice sites using *ab initio* calculations.

III. *AB INITIO* CALCULATIONS

The electronic structure of bulk palladium with different hydrogen concentrations was calculated using the *ab initio* code SIESTA.[19] We used a double-ζ polarized (DZP) basis set with the cutoff radii optimized variationally for both hydrogen and palladium and the local density approximation (LDA) to treat exchange and correlation. The real space grid cutoff (400 Ry) and the number of k points (more than 110 000) were carefully converged to achieve a very high precision and avoid spurious peaks and oscillations in the density of states. We simulated different hydrogen concentrations: PdH (100%), Pd_4H (25%), $Pd_{16}H_2$ (12.5%), $Pd_{16}H$ (6%), and $Pd_{32}H$ (3%), with the hydrogen atoms in tetrahedric and octahedric positions, and we relaxed the whole structure until the forces and the stress were small enough (0.05 eV/Å and 1 GPa, respectively). We find that the hydrogen atoms remain in the original tetrahedric or octahedric positions but the lattice is expanded. The results are shown in Table I. The octahedric configuration is always more stable than the tetrahedric, as the differences in energy between both phases $\Delta E = E_o - E_t = -0.02$, −0.08, −0.09, and −0.10 eV for PdH, Pd_4H, $Pd_{16}H$, and $Pd_{32}H$, respectively. In comparing two $Pd_{16}H_2$ cases with the hydrogen atoms in different positions, we also find that the hydrogen tends to be as separated as possible since the configuration with a separation of 2.79 Å is 0.01 eV more stable than the configuration with a separation of 1.97 Å.

Our results on the electronic properties of the PdH_x calculated for a wide range of hydrogen concentration, distributed homogeneously in tetrahedral and octahedral positions of the lattice, agree with previous theoretical

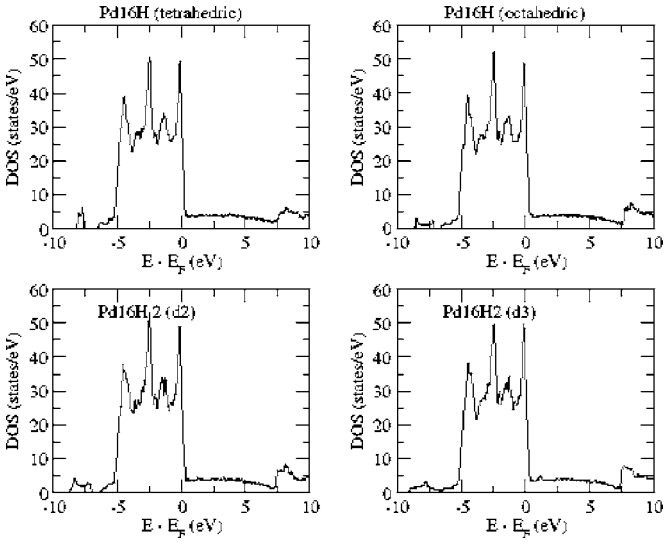

FIG. 2. The DOS for different concentrations of hydrogen in pure Pd metal.

investigations.[19,20] The DOSs we obtained are very similar to that of Gupta and Freeman,[21] Papaconstantopoulos *et al.*,[22] and Chan and Louie[13] (see Fig. 2). However, we find a distinct difference between the octahedric and the tetrahedric configurations. Hydrogen bonding with Pd is reflected through a prominent broad Pd-H band below the bottom of Pd d bands for both octahedric and tetrahedric configurations. In the former the peak below the palladium d-band complex due to the bonding with the hydrogen is rather flat and extended. In the later, however, the peak is more pronounced and localized. This means that the bonding state of hydrogen in the tetrahedric configuration does not tend to hybridize with the d states, although the form of this complex can be greatly distorted due to the lattice expansion. In our calculations the Pd-H band for octahedric site is positioned ~7.0 eV below the Fermi energy, while Chan and Louie[13] found it about 6.5 eV below the Fermi energy. The 3.0 eV width of this band in our calculations is smaller than that of Chan and Louie[13] (3.90 eV). For the tetrahedric site the peak position is located at 7.0 eV below the Fermi energy, having width less than 1.0 eV. The differences in the calculations could arise from the differences in the exchange and correlation potential. Our calculation also agrees with experimental results. X-ray photoelectron spectra of PdH by Antonangeli *et al.*[23] showed the existence of hybridized s-p-like levels of hydrogen near the bottom of the valence band, located about 6.0 eV below the Fermi energy, which is close to the band location in our calculations. The ultraviolet photoemission measurements of Eastman *et al.*[24] showed a d band of ~5.4 eV below the Fermi energy and bandwidth is about 3–4 eV wide. The other remarkable characteristic is the shift of the Fermi energy, E_F, for different hydrogen concentrations[25] (see Table I). Excluding the PdH octahedric, where the Fermi energy shifts upward relative to the Pd Fermi energy, in agreement with previous calculations, in all the remaining configurations this quantity shifts always downward and tends to the palladium value as the concentration decreases (with the clear exception of the PdH tetra-

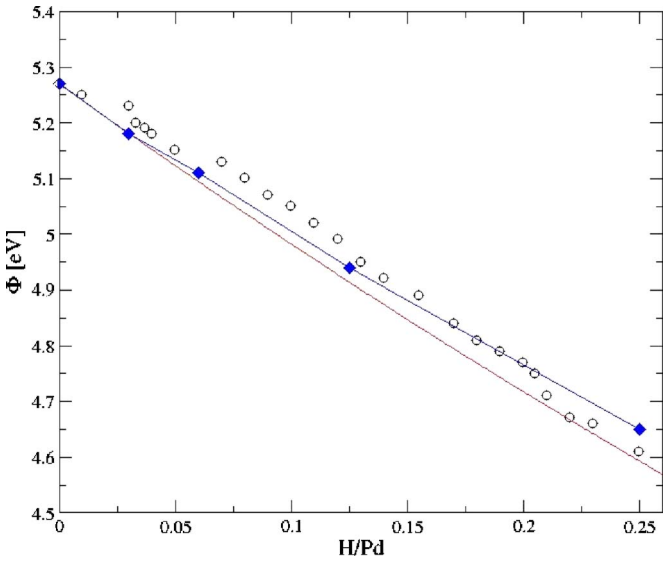

FIG. 3. (Color online) Experimental values from Ref. 29 (circles), theoretical values calculated with the metallic plasma model from Ref. 28 (continuous line), and our values calculated with the *ab initio* Fermi energies (diamonds) of the work function.

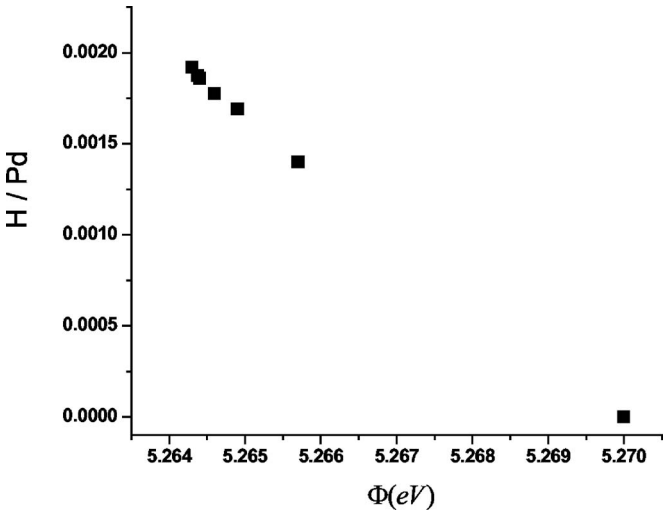

FIG. 4. Calculated values of hydrogen loading (H/Pd) in a device as a function of Φ, which is determined from the saturation currents (Fig. 1), corresponding to different values of hydrogen ppm flow rates.

hedric, which is a somewhat pathologic case). This behavior can strongly influence the electronic characteristics observed in Pd-based MIS devices, as discussed below.

IV. ROLE OF PdH FERMI ENERGY IN THE DEVICE RESPONSE

The steady-state values of the current (Fig. 1) at a fixed applied bias V_b increases with increasing ppm values of the hydrogen. The built-in potential in MIS devices due to the difference in the Fermi energy of Pd metal and semiconductor influences the current values, irrespective of the nature of the current—whether it is a diffusive, thermionic, tunneling, or their combination. Since the carrier density of the metal is many orders of magnitude larger than the semiconductor, the Fermi energy of PdH, to a larger extent, dictates the location of the equilibrium Fermi level in the energy band diagram of the whole device. From Table I we observed that the Pd's Fermi level is quite sensitive, even to the lowest concentration of hydrogen. The increasing concentration of hydrogen in Pd shifts the Fermi level downward, and this increases the steady-state value of the current as observed experimentally. However, in the capacitance measurements[6,15] of Pd-based MIS devices, the shifting Fermi level of Pd affects the depletion region of the semiconductor, thus affecting the depletion capacitance and the total capacitance of a device.

The shift in the Fermi energy[25–27] also affects the work function, Φ, of the Pd_xH surface, which we calculated using the metallic plasma model of Halas *et al.*[28] and adjusting our value of the Fermi energy for Pd to their value.[25] The results are shown in Fig. 3 for the octahedric configurations and they are in excellent agreement with previous theoretical calculations[28] and experimental measurements[29] for low concentrations of hydrogen. The changes in Φ, which decrease with hydrogen loading, strongly influence the current values in a device. Using a very general expression for the metal-semiconductor junction current, $I=I_o \exp[(\chi-\Phi)/k_BT] \times[\exp(V_b/k_BT)-1]$, we calculated the values of Φ corresponding to the experimental values of the saturation currents (Fig. 1) for different values of the hydrogen ppm flow rates and thus determine the corresponding values of hydrogen loading using data from Fig. 3. Here, I_o is some constant current, χ is the electron affinity for Si ($\chi=4.05$ eV), $T=348$ K is our measurement temperature, and the applied bias $V_b=0.6$ V. Figure 4 shows the hydrogen loading in a device as a function of Pd work function, which increases with decreasing Φ. It is interesting to note that the hydrogen ppm flow rates generally used in the Pd-based MIS devices actually represent very low concentrations of hydrogen loading (Fig. 4) in the Pd bulk. This low intake is generally attributed to the presence of defects on the device surface. At such flow rates, which represent very low hydrogen concentrations, the solid solution of hydrogen in Pd forms α phase, which is the most stable[18] phase for hydrogen concentration in the range of $0<H/Pd<0.03$. The thermodynamic concentrations of the hydrogen in the Pd are very small in our experiments due to very small values of hydrogen flow rates and our calculated phase of hydrogen is consistent with the phase presented recently by Jewell *et al.*[30] in their phase-diagram data.

In summary, we studied experimentally the current response of Pd/AlN/Si devices when exposed to different concentrations of hydrogen. For a fixed applied bias, the current showed a characteristic jump in its value when hydrogen gas is turned on. Using *ab initio* calculations, we obtained the electronic structure of bulk PdH for different hydrogen concentrations and we found that the Fermi level of PdH shifts relative to the vacuum level when the hydrogen concentration in Pd increases. The Fermi level of the PdH affects the equilibrium Fermi level of the Pd/AlN/Si device, which then directly influences the device current.

ACKNOWLEDGMENTS

This work is supported by the Smart Sensors and Integrated Microsystems (SSIM), the Institute for Manufacturing Research at Wayne State University, and the National Science Foundation (NSF) DEG-9870720 grant. The authors thank Dr. Y. Danylyuk for preparing the AlN films. V.M.G.S. thanks the EU network MRTN-CT-2004-504574 for a Marie Curie grant.

*Electronic address: jagdish@wayne.edu

[1] I. Lundström, S. Shivaraman, C. Svensson, and L. Lundqvist, Appl. Phys. Lett. **26**, 55 (1975); M. S. Shivaraman, I. Lundström, C. M. Svensson, and H. Hammarsten, Electron. Lett. **12**, 483 (1976).

[2] H. Dannetun, I. Lundstrom, and L-G. Petersson, J. Appl. Phys. **70** 453 (1991).

[3] J. W. Medin, A. H. McDaniel, M. D. Allendorf, and R. Bastasz, J. Appl. Phys. **93**(4), 2267 (2003).

[4] L. Y. Chen, G. W. Hunter, P. G. Neudeck, G. Bansal, J. B. Petit, and D. Knight, J. Vac. Sci. Technol. A **15**(3), 1228 (1997).

[5] M. Johansson, I. Lundstrom, and L-G. Ekedahl, J. Appl. Phys. **84**, 44 (1998).

[6] E. F. McCullen, H. E. Prakasam, Wenjun Mo, R. Naik, K. Y. S. Ng, L. Ramai, and G. W. Auner, J. Appl. Phys. **93**, 5757 (2003).

[7] A. Samman, S. Gebremariam, L. Ramai, X. Zhang, J. Hangas, and G. W. Auner, J. Appl. Phys. **87**, 3101 (2000).

[8] J. Fogelberg and L-G Petersson, Surf. Sci. **350**, 91 (1996).

[9] H. Dannetun, I. Lundstrom, and L-G. Petersson, J. Appl. Phys. **63**(1), 207 (1988).

[10] J. Fogelberg, M. Eriksson, H. Dannetun, and L-G Petersson, J. Appl. Phys. **78**, 988 (1995).

[11] G. W. Auner, T. Lenane, F. Ahmad, R. Naik, P. K. Kuo, and Z. L. Wu, *Wide Band Gap Electronic Materials* (Academic, New York, 1995), p. 329.

[12] F. Serina, C. Huang, G. W. Auner, R. Naik, S. Ng, and L. Rimai, Mater. Res. Soc. Symp. Proc. **622**, T12.1 (2000).

[13] C. T. Chan and S. G. Louie, Phys. Rev. B **27**, 3325 (1983).

[14] B. M. Geerken, R. Griessen, L. M. Huisman, and E. Walker, Phys. Rev. B **26**, 1637 (1982).

[15] M. Armgarth, C. Nylander, C. Svensson, and I. Lundstrom, J. Appl. Phys. **56**, 2956 (1984).

[16] M. Lischka and A. Groß, Surf. Sci. **65**, 075420 (2002); U. Muschiol, P. K. Schmidt, and K. Christmann, Surf. Sci. **395**, 182 (1998).

[17] K. Christmann, Surf. Sci. Rep. **9**, 1 (1988).

[18] J. E. Worsham, M. K. Wilkinson, and C. G. Shull, J. Phys. Chem. Solids **3**, 303 (1957).

[19] J. M. Soler, E. Artacho, J. D. Gale, A. García, J. Junquera, P. Ordejón, and D. Sánchez-Portal, J. Phys. Condens. Matter **14**, 2745 (2002).

[20] F. M. Mueller, A. J. Freeman, J. O. Dimmock, and A. M. Furdyna, Phys. Rev. B **1**, 4617 (1970).

[21] M. Gupta and A. J. Freeman, Phys. Rev. B **17**, 3029 (1978).

[22] D. A. Papaconstantopoulos, B. M. Klein, J. S. Faulkner, and L. L. Boyer, Phys. Rev. B **18**, 2784 (1978).

[23] F. Antonangeli, A. Balzarotti, A. Bainconi, E. Burattini, P. Perfetti, and N. Nistico, Phys. Lett. **55A**, 309 (1975).

[24] D. E. Eastman, J. K. Cashion, and A. C. Switendick, Phys. Rev. Lett. **27**, 35 (1971).

[25] The zero of energy is not univocally defined in an *ab initio* calculation of a bulk solid (see Ref. 26) and is typically taken as the average of the Hartree potential (see Ref. 27), which means that the absolute value of the Fermi energy is arbitrary. What matters is the difference between Fermi energies of similar calculations, where the averages of the Hartree potential, and therefore the energy references, are similar, like, for example, bulk Pd and $Pd_{32}H$. This approximation does not work for large concentrations of hydrogen and consequently, our model for the calculation of the work function makes sense for only small concentrations.

[26] L. Kleinmann, Phys. Rev. B **24**, 7412 (1981).

[27] J. Junquera, M. Zimmer, P. Ordejón, and P. Ghosez, Phys. Rev. B **67**, 155327 (2003).

[28] S. Halas, T. Durakiewicz, and P. Mackiewicz, Surf. Sci. **555**, 43 (2004).

[29] R. Duś and E. Nowicka, Langmuir **16**, 584 (2000).

[30] L. L. Jewell and B. H. Davis, Appl. Catal., A **310**, 1 (2006).